Published Online First: December, 2024
https://doi.org/10.21123/bsj.2024.10508
P-ISSN: 2078-8665 - E-ISSN: 2411-7986
Baghdad Science Journal

Theoretical calculation of radiation shielding properties of B2O3–Bi2O3–Al2O3–MgO glasses alloyed with MnO

***Shlair Ibrahim Mohammed* [1], *Zainab Qahtan Mosa*[2]**

[1] Department of Physiology, College of Medicine, University of Kirkuk, Kirkuk, Iraq.
[2]Department of Physics, College of Education for Women, University of Kirkuk, Kirkuk, Iraq
*Corresponding Author.

Received 26/12/2023, Revised 05/04/2024, Accepted 07/04/2024, Published Online First 20/12/2024

Abstract

The current work aims to calculate the gamma-ray shielding coefficients for six samples. The samples were $65B_2O_3.20Bi_2O_3.10Al_2O_3$. (5-x) MgO. xMnO ($0 \leq x \leq 1$ mol%). prepared these samples by using the melt quenching method. The study measures MAC (mass attenuation coefficient) and linear attenuation coefficient (μ_m, μ). It also calculates the halve-value layer, ten-value layer (TVL), and mean free path (MFP). The calculation was conducted using the Phy-X/PSD and XCOM programs, in an energy range 1keV- 100GeV. The study discusses comparing the results with each other showing a good agreement. The study has shown many results such as when the energy is higher than 10 MeV. There were many peaks in the low photon energy region (< 0.1 MeV). The glass sample with the biggest MnO composition S6 shows many peaks at the M-, L-, and K- absorption photoelectric edges. The measured values that Phy-X/PSD and XCOM software produced showed good agreement. Also, there is a negative correlation between the HVL and material density. In addition, MFP and HVL values begin low and continuously increase as the incident energy of the photon rises to 5 MeV. Beyond 5 MeV, with energies, HVL and MFP dropped softly. Half-Value Layer values drop with the rise in the density and MnO contents.

Keywords: Protection properties; Glass; Photon attenuation- coefficient; Half value layer; Tenth value layer; XCOM; Phy-X/PSD.

Introduction

Knowledge of shielding properties such as the coefficient of total linear- attenuation μ, coefficient of mass attenuation ($\mu_m=\mu/\rho$), mean free path (MFP), Tenth value layer (TVL), half value layer (HVL) and is essential in the domain of radiation physics [1-3]. shielding materials are used to control radiation exposure of Neutrons and gamma rays [4]. A radiation beam experiences attenuation when it enters a bodily part; the degree of attenuation varies with the medium's thickness and density[5]. Protective barriers and shields are used to reduce the dose of radiation exposure to people working in the field of radioactive sources[6]. Concrete and building materials are frequently employed as radiation protection materials due to their low cost and flexibility to be molded to any mason design [7,8]. However, concrete has various restrictions, including the addition of humidity content, being opaque to losing water, visible light, and incisions development [9]. Because of these constraints, a stronger shielding material is required. Glass is a better radiation shielding material than concrete [7,10]. Heavy metal oxide-containing glasses, such as Bi_2O_3 and PbO, may significantly absorb gamma-ray and are one of the conceivable

Published Online First: December, 2024
https://doi.org/10.21123/bsj.2024.10508
P-ISSN: 2078-8665 - E-ISSN: 2411-7986
Baghdad Science Journal

substitutes for concrete [11,12]. The authors have selected bismuth oxide as the material for preparing the shielding, Due to the toxic action of lead. Because of their greater density and refractive index values, bismuth borate glasses have sparked a lot of attention [13]. B_2O_3 is a good glass mold in trigonal [BO_3] /tetrahedral [BO_4] units On the other hand, Bi_2O_3 is affiliated with the denomination of conditional glass makers. It behaves as a modifier at low concentrations and the former at high concentrations [14]. In this study, We employed the software Phy-X/PSD to examine the photon protection characteristics of gamma for systems of $65B_2O_3.20Bi_2O_3.10Al_2O_3.(5\text{-}x)MgO.xMnO$ glass [15].

Materials and Methods

The $65B_2O_3.20Bi_2O_3.10Al_2O_3.(5\text{-}x)MgO.\ xMnO$ glasses' chemical composition, concentration, and densities were acquired [15], which is six samples of glass like those described in Table 1. which shows that as the concentration of the MgO decreases from 5 to 4 mol% the MnO concentration increases from 0 to 1 mol%. The software Phy-X / PSD enhanced by Şakar et al. is able to be utilized as open-source code and online. Phy-X / PSD program was created with the runtime environment Node.js v8.4.0Nginx 1.15.8 enhance security between the server and the client browser. The communication between the server and client browsers is secured using Positive SSL 256-bit encryption. It can calculate numerous shielding factors at various energies [16]. The Phy-X/PSD system rapidly and precisely evaluates the attenuation parameters, allowing the user to store the estimated values in an Excel dossier conveniently. The computations are broken down into three stages: (i) Materials definition: the weight fraction, sample density, and mole fraction are all entered. (ii) The energies are chosen from two specified ranges: 1 keV to 100 GeV and 15 keV to 15 MeV. In Phy-X/PSD, there are other readily accessible radioactive sources and energies that are widely recognized. (iii) Setting the properties: 18 protection properties can be counted, including μ, μ_m, TVL, MFP, and HVL[15]. XCOM is a mixed rule-based software or dataset. It may provide mass coefficient attenuation for various elements within a specific energy range from 1 keV to100 GeV for various interaction processes such as coherent and incoherent scattering, pair production, and photoelectric-absorption. Generally, the Lambert-Beer rule describes the coefficient of mass-attenuation of the samples as shown in Eq 1[17].

$$\mu_m = \sum_{i=1}^{n} w_i \mu_m = \frac{\mu}{\rho} \quad (1)$$

Where w_i and μ_m are, respectively, the fraction by weight of i^{th} of n elements contained in the glass and the mass attenuation coefficient.

The mean free- path (MFP) denotes the average traveled distance that a photon travels before undergoing a collision. The half-value layer (HVL) refers to the thickness of a substance at which 50% of the intensity of a photon incident has been reduced. HVL and MFP can be explained as [18–20]:

$$MFP = \left(\frac{1}{\mu}\right) \quad (2)$$

$$HVL = \frac{0.693}{\mu} \quad (3)$$

Here, μ represents the linear- attenuation coefficient (LAC).

Table 1. The density and the chemical compositions of $65B_2O_3.20Bi_2O_3.10Al_2O_3.(5\text{-}x)MgO.\ xMnO$ ($0 \leq x \leq 1$)

Sample code	B_2O_3	Bi_2O_3	Al2O3	MgO	MnO	Density (g/cm3)
S1	65	20	10	5	0	4.900
S2	65	20	10	4.8	0.2	4.917
S3	65	20	10	4.6	0.4	4.928
S4	65	20	10	4.4	0.6	4.938
S5	65	20	10	4.2	0.8	4.961
S6	65	20	10	4	1	4.970

Published Online First: December, 2024
https://doi.org/10.21123/bsj.2024.10508
P-ISSN: 2078-8665 - E-ISSN: 2411-7986
Baghdad Science Journal

Results and Discussion

The study has calculated many features such as the coefficient of linear attenuation (LAC), coefficient of mass attenuation (MAC), MFP, HVL, and TVL by the use of the XCOM and Phy-X/PSD programs. XCOM and Phy-x programs were used to measure the MAC (mass attenuation- coefficient). MAC coefficient of mass attenuation drops continuously with an energy photon, the Phy-X/PSD software and XCOM values for a specific sample in the range of energy 1 keV to 100 GeV showed that there was a negative correlation between the photon energies and the mass attenuation and linear attenuation of the glass samples. This is because higher energy photons have a greater tendency to interact with the electrons in the material, causing electron emission and the formation of defects[21]. This arises from when the radiation interacts with matter and energy[22]. The photon interacts with matter in three ways: the photoelectric effect at low energies (less than 100 keV), pair production at high energies (above 10^6 keV), and Compton scattering occurs at medium energies (between 10^2-10^6 keV). The MAC values are calculated by the Phy-X/PSD software as in Fig 1.

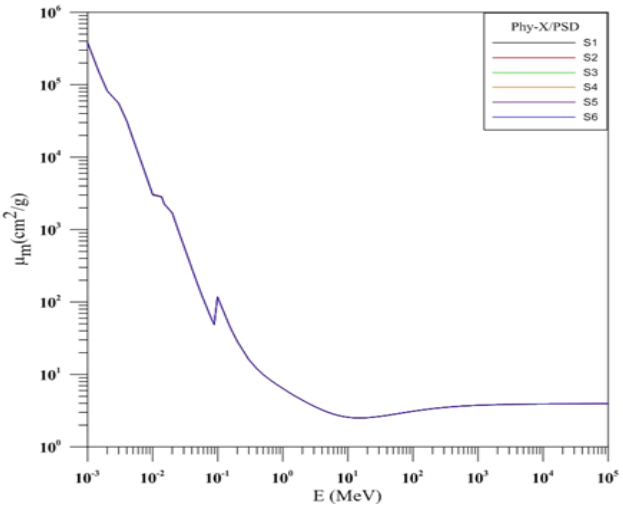

Figure 1. The Phy-X/PSD program provides the μ_m mass-attenuation coefficient values for calculated data samples.

Then, they quickly dropped to a depressed energy range of 1 keV < E < 100 keV, the value is biggest if the energy becomes higher than 100 keV owing to the K-absorption brim of element (MnO). All μ_m sample values are in the range of 1 to 0.06 $cm^2.g^{-1}$, So, in a low-energy region, the MAC value drops quickly, if the scattering Compton dominates. When the energy is higher than 10 MeV, There were many peaks at low photon energy region (< 0.1 MeV). This work examines the MnO concentricity trace on the shielding features of $65B_2O_3.20Bi_2O_3.10Al_2O_3$. (5-x) MgO.xMnO system of glass. The total MAC, from the calculation, is seen as the MnO% concentration function in Figs 1, 2.

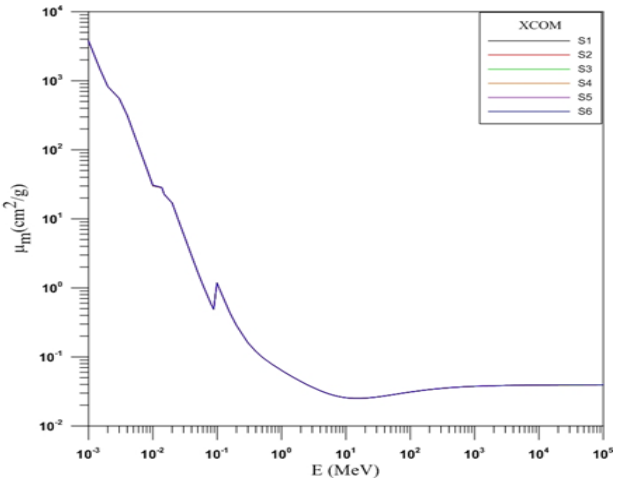

Figure 2. The XCOM software values of μ_m the total mass-attenuation coefficient estimated glass samples.

Increasing the MnO concentration raises the mass attenuation coefficient showing that μ_m of $65B_2O_3.20Bi_2O_3.10Al_2O_3$. (5-x) MgO. xMnO system was 0.0982 $cm^2.g^{-1}$ and decreased to 0.098 $cm^2.g^{-1}$ at 511 keV for radioactive source as seen in (table 2) ^{22}Na, and at ^{137}Cs from 0.098224 $cm^2.g^{-1}$ to 0.098221 $cm^2.g^{-1}$ at 662 keV as the MgO concentration decrease [23]. A study very well confirmed the measured values that Phy-X/PSD and XCOM software produced. The current work examined the MnO concentration impact on the shielding features of the $65B_2O_3.20Bi_2O_3.10Al_2O_3$. (5-x)MgO.xMnO glass system.

Published Online First: December, 2024
https://doi.org/10.21123/bsj.2024.10508
P-ISSN: 2078-8665 - E-ISSN: 2411-7986
Baghdad Science Journal

Table 2. The mass attenuation coefficient of $65B_2O_3.20Bi_2O_3.10Al_2O_3.(5-x)MgO.\ xMnO\ (0 \leq x \leq 1)$

Energy	511keV	511keV	662keV	662keV
Sample code	Phy-x/PSD	XCOM	Phy-x/PSD	XCOM
S1	0.0982204	0.09822	0.0822686	0.08224
S2	0.098213	0.09821	0.08226088	0.08224
S3	0.0982056	0.09821	0.08225315	0.08223
S4	0.0981982	0.0982	0.08224543	0.08222
S5	0.0981908	0.09819	0.08223771	0.08221
S6	0.0981834	0.09818	0.08222999	0.08221

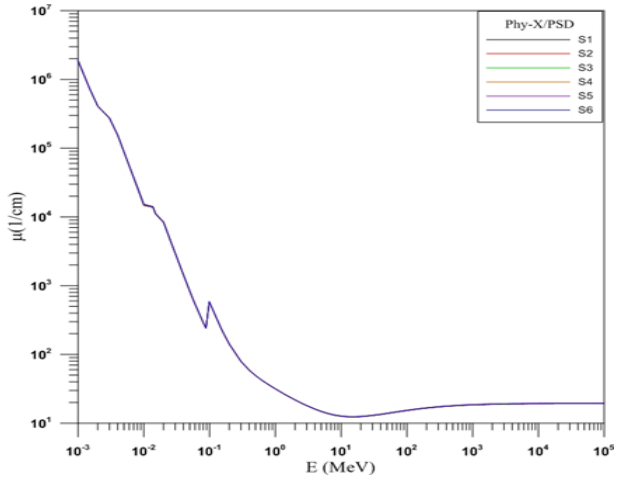

Figure 3. Phy-X/PSD Software values of the linear-attenuation (μ) for the samples of glass.

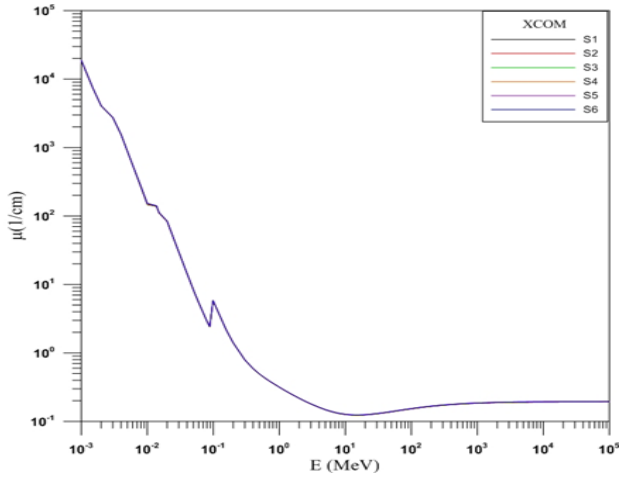

Figure 4. The XCOM program values of the linear- attenuation (μ) for the glass samples

Figs 1-4, shows the calculated μm & μ values as a function of MnO% concentration. Also, the mass & linear attenuation coefficients positively correlate with the MnO concentration and the 65B2O3.20Bi2O3.10Al2O3. (5-x) MgO.xMnO glass system rises with the rise of the density of the material[24]. Eq 1 shows the inverse relation between MAC and density.

An (HVL) half Value-Layer of the checked samples ranges between 1 keV and 100 GeV. In contrast, there was a negative correlation between the MnO concentration and the HVL. Eq 3 shows that there is an inverse link between HVL and the LAC, as illustrated in Figs 5,6. HVL increases gradually as the input photon energy increases for a range of energies[25]. The HVL of the glasses S1 increased from 0.022063584 to 0.045658202 cm, while it increased from 0.021764941 to 0.044812375 cm for S6 at photon energies (1- 100 MeV). A study shows that the HVL readings of the last sample (S6) were smaller values because of the MnO concentration. Also, there is a negative correlation between the HVL and material density. Figs 5- 8, depict the computed mean free path (MFP) and HVL values for the glass samples with a range of 1 keV to 100 GeV of energies. In addition, it has been discovered that the MFP and HVL values start low and progressively rise as the incident photon energy increases up to 5 MeV. Beyond 5 MeV, reaching these energies, HVL and MFP dropped slightly, the rate at which MFP and HVL are decreasing is sluggish as incident energy increase. Half-Value Layer values drop with the rise in the density and MnO contents as obtained in Ref.[26]. The photon-matter interaction mechanisms outlined for the ($\mu/\rho=\mu_m$) can be referred to as the current HVL behavior for these glass samples.

Published Online First: December, 2024
https://doi.org/10.21123/bsj.2024.10508
P-ISSN: 2078-8665 - E-ISSN: 2411-7986
Baghdad Science Journal

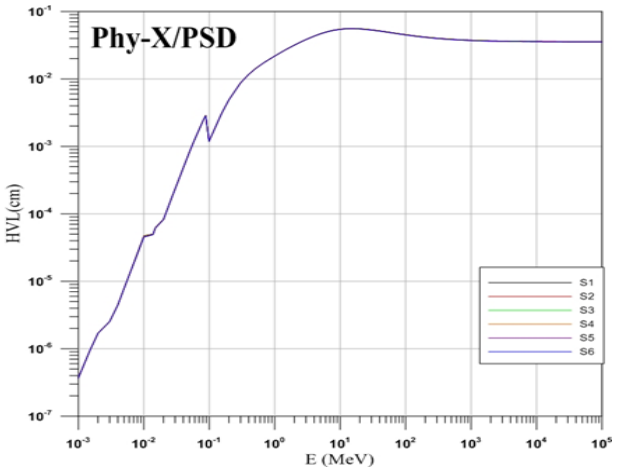

Figure 5. The half-value layer of the selected samples with the energy of a photon, calculated by Phy-X/PSD.

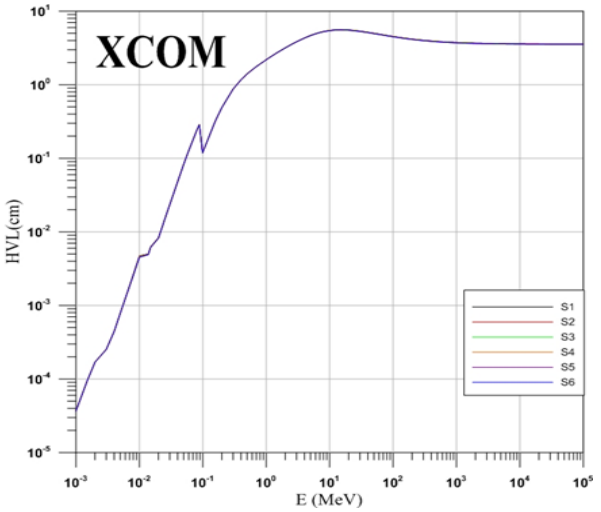

Figure 6. The half-value layer of the selected samples with the energy of a photon, calculated by the XCOM program.

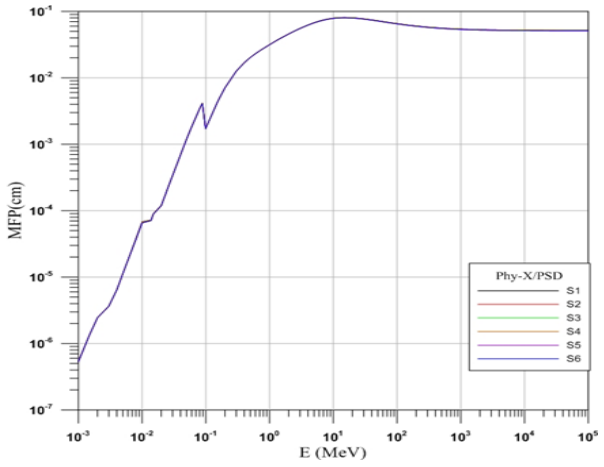

Figure 7. Shows the mean free path (MFP) of the chosen samples using the Phy-X/PSD program.

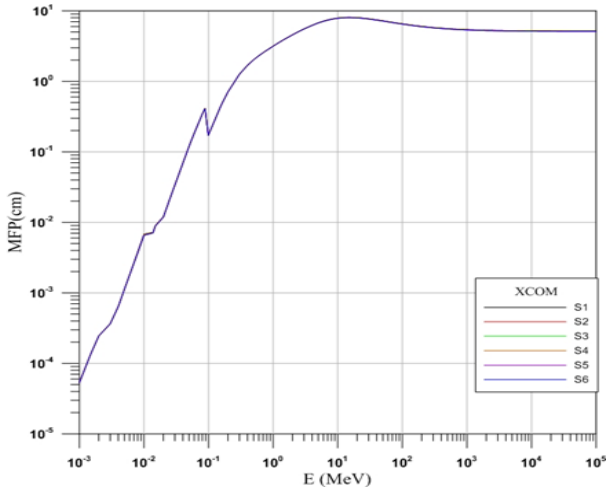

Figure 8. The XCOM program was used to determine the variation of the (MFP) of the selected samples.

When higher than 5MeV, the drop in the HVL and MFP is slight with the incident energy. Also, there is a clear rise in the MnO concentration and density decreasing HVL and MFP values. Furthermore, the sample S6 absorption edges are lower than those of the other samples. TVL (tenth-value layer) values calculated for the glass investigated samples by XCOM and Phy-x at the range (1 keV-100GeV) are clarified in Figs 9,10. The values of TVL were found low initially and with the increase in energy incident photons gradually increased. Where the sample edge

Published Online First: December, 2024
https://doi.org/10.21123/bsj.2024.10508
P-ISSN: 2078-8665 - E-ISSN: 2411-7986
Baghdad Science Journal

S1 was found greater than the first edge of S6[23]. Good agreements between the calculated values.

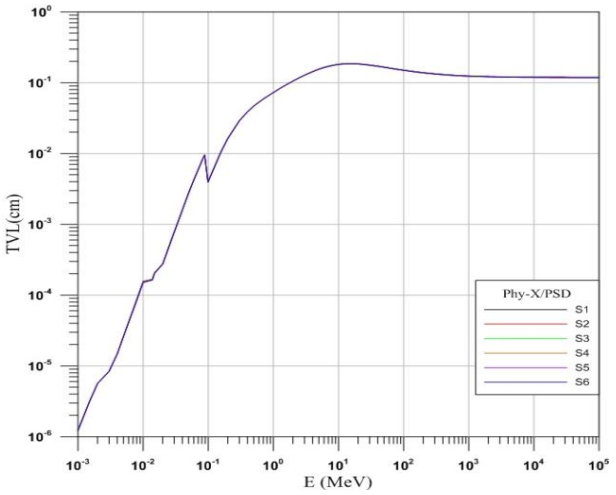

Figure 9. Tenth-value layers of the chosen samples measured by Phy-X/PSD.

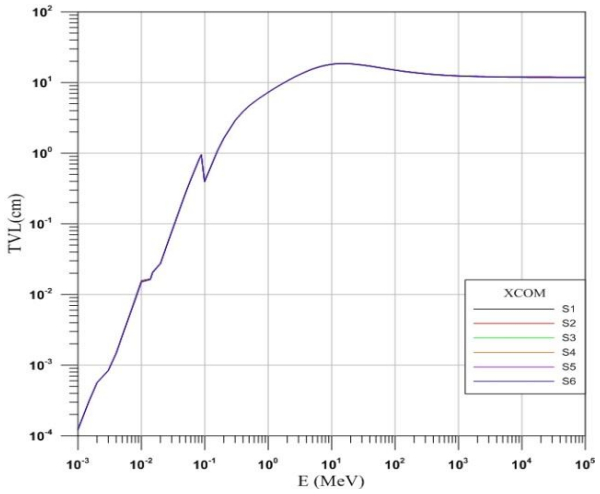

Figure 10. Tenth-value layers of the chosen samples measured by XCOM.

Conclusion

Some of the gamma-ray attenuation parameters were calculated for glass samples with a gamma energy range of 1kev-100Gev utilizing the Phy-X/PSD and XCOM programs. It was found that the mass-attenuation coefficient (MAC) and the linear-attenuation coefficient (LAC) concentrations increased as MgO and MnO decreased and increased respectively[24]. However, the HVL and MFP, both rise as the amount of MnO increases and the amount of MgO decreases. It was found that the values of MAC and LAC tend to fall as the photon energy increases, whilst halve-value layer, ten-value layer (TVL) and mean free path (MFP) increase. Due to lower HVL values ($1.065*10^{-6}$-0.05cm) and values of MFP, the S6 glass system demonstrates superior protective capacity compared to the other glass samples in $65B_2O_3$–$20Bi_2O_3$–$10Al_2O_3$-(5-x)MgO-xMnO systems ($1.54*10^{-6}$–0.07cm). While the mass-attenuation coefficient is at its highest for the S6 sample which contains 4 (mol%) MgO and 1 (mol%) MnO, the (MAC) values for S6 glass range from 130922.6091 –2.71 $cm^2.g^{-1}$, and the gamma rays' energy varies from 1 keV to 100 GeV. The S6 specimen of top density offers better photon protection capabilities due to its low values of TVL (tenth-value layer), (half-value layer) HVL, and MFP (mean free path), as well as its high LAC (coefficient of linear-attenuation) and MAC (coefficient of mass attenuation) values. All values of μ_{Phy-x} are slightly greater than the μ_{XCOM} values. The mass-attenuation values obtained from both methods confirmed the accuracy of the current Phy-X/PSD. The study proved that the sixth sample provides the best protection against gamma rays, so it can be used to protect against radiation. It was calculated in two ways to further confirm that it can be used in γ-ray shielding.

Authors' Declaration

- Conflicts of Interest: None.
- We hereby confirm that all the Figures and Tables in the manuscript are ours. Furthermore, any Figures and images, that are not ours, have been included with the necessary permission for re-publication, which is attached to the manuscript.
- No animal studies are present in the manuscript.
- No human studies are present in the manuscript.

Published Online First: December, 2024
https://doi.org/10.21123/bsj.2024.10508
P-ISSN: 2078-8665 - E-ISSN: 2411-7986
Baghdad Science Journal

- Ethical Clearance: The project was approved by the local ethical committee at University of Kirkuk.

Authors' Contribution Statement

This work was carried out in collaboration between all authors. Sh. I. M. collected the samples and wrote and edited the manuscript with revisions ideas. Z. Q. M., analysis of the data with revision idea

References

1. Sukhpal S, Ashok K, Devinder S, Kulwant S T, Gurmel S. Barium – borate – flyash glasses: as radiation shielding materials. Nucl Inst Methods Phys Res. 2008; 266: 140–146. https://doi.org/10.1016/j.nimb.2007.10.018
2. Sayyed M.I. Bismuth modified shielding properties of zinc boro-tellurite glasses. J Alloys Compd. 2016; 688: 111–117. https://doi.org/10.1016/j.jallcom.2016.07.153.
3. Sayyed M.I. Investigation of shielding parameters for smart polymers. Chin J Phys. 2016; 54(3): 408–415. https://doi.org/10.1016/j.cjph.2016.05.002
4. Vishwanath P S, Badiger NM, Kaewkhao J. Radiation shielding competence of silicate and borate heavy metal oxide glasses: comparative study. J Non-Cryst Solids. 2014; 404: 167–173. https://doi.org/10.1016/j.jnoncrysol.2014.08.003
5. Shafik SS, Basim KR, Rajiha RM, Wijdan TF. Study the Shielding Properties against Gamma-rays for Epoxy Resin Reinforced by Different materials. Baghdad Sci J. 2011; 8(3): 705-710. https://doi.org/10.21123/bsj.2011.8.3.705-710.
6. Samer K Y, Laith Abd Al-Aziz A. Impact of geometric factor in accumulation factor measurements of gamma rays. Baghdad Sci J. 2021; 2(4): 6-623. https://doi.org/10.21123/bsj.2005.659
7. Kaundal RS, Sandeep K, Narveer S, Singh KJ. Investigation of structural properties of lead strontium borate glasses for gamma ray shielding applications. J Phys Chem Solids. 2010; 71(9): 1191–1195. https://doi.org/10.1016/j.jpcs.2010.04.016.
8. Mostafa AM, Shams AM, Sayyed MI. Gamma ray shielding properties of PbO-B2O3-P2O5 doped with WO3. J Alloys Compd. 2017; 708: 294–300. https://doi.org/10.1016/j.jallcom.2017.02.303.
9. Sandeep K, Singh KJ. Investigation of lead borate glasses doped with aluminum oxide as gamma ray shielding materials. Ann Nucl Energy. 2014; 63: 350–354. https://doi.org/10.1016/j.anucene.2013.08.012.
10. Tuscharoen S, Kaewkhao J, Limkitjaroenporn P, Limsuwan P, Chewpraditkul W. Improvement of BaO: B2O3: fly ash glasses: radiation shielding, physical and optical Properties. Ann Nucl Energy. 2012; 49: 109–113. https://doi.org/10.1016/j.anucene.2012.05.017 .
11. Singh K, Singh N, Kaundal R, Singh K. Gamma-ray shielding and structural properties of PbO-SiO2 glasses, Nucl Instrum Methods Phys Res B. 2008; 266(6): 944-948. https://doi.org/10.1016/j.nimb.2008.02.004.
12. Ashok K. Gamma ray shielding properties of PbO-Li2O-B2O3 glasses. Radiat Phys Chem. 2017; 136: 50-53. https://doi.org/10.1016/j.radphyschem.2017.03.023.
13. Isabella-Ioana O, Hartmut H, Klaus B. Optical properties of bismuth borate glasses, Opt Mater. 2004; 26(3): 235-237. https://doi.org/10.1016/j.optmat.2003.10.006.
14. Thomas M. Review of Bi2O3 based glasses for electronics and related applications. Int Mater Rev. 2013; 58(1): 3-40. https://doi.org/10.1179/1743280412Y.0000000010
15. Krishna G P, Yusub S, Ramesh B A, Sree N R, Aruna V. Electrical and spectroscopic characteristics of B2O3–Bi2O3–Al2O3–MgO glasses alloyed with MnO. J Phys Chem Solids. 2022; 170: 110957. https://doi.org/10.1016/j.jpcs.2022.110957
16. Şakar E, Özpolat OF, Alım B, Sayyed MI, Kurudirek M. Phy-X / PSD: Development of a user friendly online software for calculation of parameters relevant to radiation shielding and dosimetry. Radiat Phys Chem. 2020; 166: 108496. https://doi.org/10.1016/j.radphyschem.2019.108496.
17. Ali H T, Qahtan A M, Gulalla A K. Study of the properties of soil in Kirkuk, Iraq. J Radiat Res Appl Sci. 2016; 9: 256-265. https://doi.org/10.1016/j.jrras.2016.02.006
18. Ali H Taqi, Abdulahdi M, Ghalib S, Mohammed I. Shielding Properties of Glass Samples Containing Li2O, K2O, Na2O, PbO and B2O3 by Geant4, XCOM and Experimental Data. Jordan J Phys. 2022; 15: 331-341. https://doi.org/10.47011/15.4.1
19. Sayyed MI, El-Mallawany R. Shielding properties of (100 −x) TeO2-(x) MO3 glasses. Mater Chem Phys. 2017; 201: 50–56. https://doi.org/10.1016/j.matchemphys.2017.08.035
20. Dong NG, El-Mallawany R, Sayyed MI, Tekin HO. Shielding properties of 80TeO2–5TiO2–(15 −x) WO3–xAnOm glasses using WinXCom and MCNP5 code. Radiat Phys Chem. 2017; 141: 172–178. https://doi.org/10.1016/j.radphyschem.2017.07.006
21. Amani A, Al Huwayz M, Alrowaili ZA, Al-Buriahi MS. Radiation attenuation of SiO2–MgO glass system

Published Online First: December, 2024
https://doi.org/10.21123/bsj.2024.10508
P-ISSN: 2078-8665 - E-ISSN: 2411-7986
Baghdad Science Journal

for shielding applications. J Radiat Res Appl Sci. 2023; 16(4): 100746. https://doi.org/10.1016/j.jrras.2023.100746
22. Amal A EL-Sawy, Madbouly AM. Comparative Study of Gamma Radiation Shielding Parameters for Different Oxide Glasses. Eur Acad Res. 2018; VI (2): 824. https://doi.org/10.13140/RG.2.2.13185.10089
23. Ali H T. Ali IS, Azeldeen H I. Electromagnetic-Ray Absorption Using B2O3-PbO-Na2O Glass Mixtures as Radiation Protection Shields. Arab J Nucl Sci Appl. 2021; 25(1): 53-61. http://dx.doi.org/10.21608/ajnsa.2021.74814.1469 .
24. Almisned G, Iskender A, Huseyin O T, Ismail Yuksek, İsmail Ekmekçi. Variation in gamma ray shielding properties of glasses with increasing boron oxide content. Radiochimica Acta. 2022; 111(3): 217-223. https://doi.org/10.1515/ract-2022-0108
25. Hanfi MY, Sayyed MI, Lacomme E, Akkurt I, Mahmoud KA. The influence of MgO on the radiation protection and mechanical properties of tellurite glasses. Nucl Eng Technol. 2021; 53: 2000:2010. https://doi.org/10.1016/j.net.2020.12.012
26. Al-Hadethi Y, Sayyed MI, Tijani SA. Gamma Radiation Attenuation Properties of Tellurite Glass: A comparative study. Nucl Eng Technol. 2019; 51(8): 2005-2012. https://doi.org/10.1016/j.net.2019.06.014

الحساب النظري لخصائص التدريع الإشعاعي للزجاج $B_2O_3–Bi_2O_3–Al_2O_3–MgO$ المخلوط بـ MnO

شلير ابراهيم محمد [1]، زينب قحطان موسى[2]

[1] فرع الفسلجة ، الكلية الطب، الجامعة كركوك، كركوك، العراق.
[2]القسم الفيزياء، الكلية التربية للبنات، الجامعة كركوك، كركوك، العراق

الخلاصة

يهدف العمل الحالي الى حساب معاملات التدريع أشعة جاما لستة عينات. $65B_2O_3.20Bi_2O_3.10Al_2O_3.$ (5-x) MgO. xMnO ($0 \leq x \leq 1$ mol%). العينات,تم تحضير هذه العينات باستخدام طريقة ذوبان تبريد. تقيس الدراسة معاملات التوهين الكتلية والخطية (μ_m, μ). كما يقوم أيضًا بحساب طبقة القيمة النصفية، وطبقة القيمة العشرة (TVL)، ومتوسط المسار الحر (MFP). تم إجراء الحساب باستخدام برامج Phy-X/PSD وXCOM، في نطاق طاقة 1keV-100GeV. وتناقش الدراسة النتائج المحسوبة مع بعضها االبعض وقد لوحظت أتفاق جيدا. وقد أظهرت الدراسة العديد من النتائج مثل أنه عندما تكون الطاقة أعلى من 10 MeV، فإن إجمالي MAC يرتفع ويستقر عندما يقرب من 400 MeV. كانت هناك العديد من القمم في منطقة طاقة الفوتون المنخفضة (<0.1 MeV). تُظهر عينة الزجاج التي تحتوي على أكبر تركيبة MnO S6 العديد من القمم عند حواف الامتصاص الكهروضوئية M وL وK. أظهرت القيم المقاسة التي أنتجها برنامج Phy-X/PSD وXCOM توافقًا جيدًا. أيضا، هناك علاقة سلبية بين HVL وكثافة المواد. بالإضافة إلى ذلك، تبدأ قيم MFP وHVL منخفضة وتزداد باستمرار مع ارتفاع الطاقة الساقطة للفوتون إلى 5 MeV. بعد 5 MeV ، مع زيادة الطاقات، انخفض HVL وMFP بهدوء. تنخفض قيم طبقة نصف القيمة مع ارتفاع الكثافة ومحتو MnO

الكلمات المفتاحية: الكلمات المفتاحية: خصائص الحماية، زجاج، معامل توهين الفوتون، طبقة نصف القيمة، طبقة القيمة العاشرة، Phy-X/PSD،XCOM .